Monitoring Pulsed Power on Ship Electrical Systems[1]

George L. Kusic[2] , John M. Heinzel[3], Donald J. Hoffman[4]

Abstract – **In this paper, forthcoming distributed generation and energy storage systems for ships are monitored by Sampled State Estimation (SSE). The paper demonstrates how a high data rate from transducers on the electrical system can be used in a discrete version of State Estimation that is effective in transient conditions as well as in steady operation. Various energy storage devices such as batteries are distributed around the ship and employed in conjunction with rotating machine generation in order to deliver pulses of power that far exceed the capability of the rotating machines. The distributed energy storage is coordinated to serve high pulse loads and employed to service local loads via dc/dc or dc/ac converters for fail-safe local power operation. The advantages of State Estimation on ship power systems are demonstrated for sampled data from current and voltage transducers.**

Keywords – **State Estimation, Sampled Data, Transient Operation, Pulsed Power, Ship Survivability**

I. Introduction

In a compact ship's power system there is essentially synchronization of high rate data from transducers, so voltage and current measurements are a 'snapshot' of the power system and can be used to detect bad measurements.

Ship's power systems are increasingly distributed and complex with ac and dc converter-coupled buses and energy storage such as batteries, flywheels, compressed air, high temperature superconducting coils, super-capacitors, fuel cells, and others. The distributed storage devices can be coordinated to deliver large amounts of power to high-power loads such as rail launchers, electromagnetic pulses, or sudden ship propulsion manoeuvres. The rotating machines are used as pulsed power sources [1-3], but there are current limits caused by sub-transient inductances. One estimate is that pulse power for a rail gun requires 1.35 GW peak and 19MW average power over a 4 Second transient [4]. These pulse requirements are significant considering that the ship requires on the order of 90% of its 40 MW generation for propulsion [5]. There are also stability problems [6] that may limit pulsed power. As a consequence, batteries and directly coupled energy sources are significant because they have high short circuit current capability and their limitation is primarily the line impedance between them and the pulsed load.

[1]Sponsored by U.S. Navy NSWCCD Grant #N00014-12-1-0891
[2]George L. Kusic is with the Department of Electrical Engineering at the University of Pittsburgh, Pittsburgh, PA, 15261, USA e-mail: **kusic@engr.pitt.edu**
[3]John. M. Heinzel is with the U.S. Navy CIV NSWCCD, Philadelphia, PA 9850 e-mail **john.heinzel@navy.mil**
[4]Donald J. Hoffman is with the U.S. Navy CIV NSWCCD, Philadelphia, PA 9850 e-mail **donald.hoffman@navy.mil**

As batteries and directly-coupled devices are employed for pulsed power, their transient response must be monitored for source degradation and energy contribution. For example, the state of charge of a battery in a transient during a uniformly sampled interval is given by Eq. 1.

$$Q_e(t) = Q_{initial} - \int_0^{K\Delta t} i(t)dt \cong Q_{initial} - \sum_{k=1}^{K} i_k \Delta t \qquad (1)$$

In order to monitor the electrical system during pulses or transients, an extension of State Estimation (SE) is to be used. SE is a well-known real time monitor for earth power systems to provide a smoothed data analysis of voltages, currents, power flow that is free from sensor measurement errors. SE computed results are normally presented on computer screens to operators of the power system. The computed results process data far in excess of human capability and virtually instantaneously provide 'smoothed' estimates of the power system operating point. A primary feature of SE is that is that redundancy in data allows bad data detection, such as when an A/D transducer or its communication channel fails.

For earth power systems, analog data from the circuit breakers, line power transducers, current measurements, etc. is collected from sensors distributed over the system, digitized, and then transmitted to the central computer. SE [7] for earth systems is least-squares fit of real power and reactive power measurements to calculate the phase angle of 60 Hz bus voltages and magnitudes of the voltages. Power flow is typically averaged over several cycles of the 60 Hz line waveform. Because directly measured voltages and currents lack synchronization, they are not used in earth systems because they cause the SE calculation to diverge [8].

For a ship's power system, fiber optic transmission of digital data is the logical choice because it supports a high data rate, has noise immunity, is light weight, and has electrical isolation. The other feature of the ship's data acquisition system is that data is synchronized and hence corresponds to a true time **'snapshot'** of the electrical power system.

II. Ship Power System State Estimation by Discrete Samples

Any electrical line, dc or 3-phase ac, connected between two points (called buses) can be modelled to a first approximation by the pi-equivalent circuit shown in Fig. 1.

Report Documentation Page

Form Approved
OMB No. 0704-0188

1. REPORT DATE	2. REPORT TYPE	3. DATES COVERED
APR 2013	**N/A**	**-**

4. TITLE AND SUBTITLE	5a. CONTRACT NUMBER
Monitoring Pulsed Power on Ship Electrical Systems	5b. GRANT NUMBER
	5c. PROGRAM ELEMENT NUMBER
6. AUTHOR(S)	5d. PROJECT NUMBER
	5e. TASK NUMBER
	5f. WORK UNIT NUMBER
7. PERFORMING ORGANIZATION NAME(S) AND ADDRESS(ES) **Department of Electrical Engineering at the University of Pittsburgh, Pittsburgh, PA, 15261, USA**	8. PERFORMING ORGANIZATION REPORT NUMBER
9. SPONSORING/MONITORING AGENCY NAME(S) AND ADDRESS(ES)	10. SPONSOR/MONITOR'S ACRONYM(S)
	11. SPONSOR/MONITOR'S REPORT NUMBER(S)

12. DISTRIBUTION/AVAILABILITY STATEMENT
Approved for public release, distribution unlimited

13. SUPPLEMENTARY NOTES
See also ADA581781. IEEE Electric Ship Technologies Symposium (IEEE ESTS 2013) Held in Arlington, Virginia on April 22-24, 2013. U.S. Government or Federal Purpose Rights License.

14. ABSTRACT
In this paper, forthcoming distributed generation and energy storage systems for ships are monitored by Sampled State Estimation (SSE). The paper demonstrates how a high data rate from transducers on the electrical system can be used in a discrete version of State Estimation that is effective in transient conditions as well as in steady operation. Various energy storage devices such as batteries are distributed around the ship and employed in conjunction with rotating machine generation in order to deliver pulses of power that far exceed the capability of the rotating machines. The distributed energy storage is coordinated to serve high pulse loads and employed to service local loads via dc/dc or dc/ac converters for fail-safe local power operation. The advantages of State Estimation on ship power systems are demonstrated for sampled data from current and voltage transducers.

15. SUBJECT TERMS

16. SECURITY CLASSIFICATION OF:			17. LIMITATION OF ABSTRACT	18. NUMBER OF PAGES	19a. NAME OF RESPONSIBLE PERSON
a. REPORT	b. ABSTRACT	c. THIS PAGE			
unclassified	**unclassified**	**unclassified**	**SAR**	**8**	

Instantaneous voltages V_i and V_j in Fig. 1 are called the 'State' of the power system. Current into the line at bus *i* is:

$$I_i = C\partial V_i / \partial t + I_{iS} \quad (2)$$

where I_{iS} is in the series the current flow in the pi-line computed from:

$$V_i - V_j = RI_{iS} + L\partial I_{iS} / \partial t \quad (3)$$

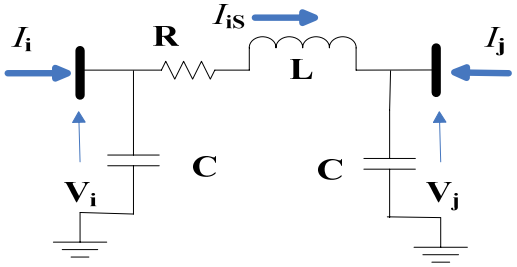

Fig. 1 Pi-equivalent of a transmission line (R, L, C, 2-conductor elements or symmetrical component equivalents of matrices in three-phase analysis)

The first order Euler finite difference approximation to both eqs. (2) and (3) at the kth and (k-1)th instants of time is:

$$I_i(k) = C[V_i(k) - V_i(k-1)] / \Delta t$$
$$+ \left[R + L/\Delta t\right]^{-1}\left[V_i(k) - V_j(k) + LI_{iS}(k-1)/\Delta t\right] \quad (4)$$

where the uniform time step is Δt. These equations march in time, so a starting value is necessary. If the voltages have been determined, then the currents on the transmission line can be calculated.

For a general ungrounded ship power network, voltages are measured line-to-line, the currents in the transmission lines are measured, and if multiple lines meet at a bus (point), the currents into the bus are called injection currents. Samples of measured currents and voltages are collected, digitized, accumulated, and sent as a data 'snapshot' to the State Estimator. The example network shown in Fig. 2 indicates the points where voltages and currents are measured.

Measurements performed on the network are used to calculate the instantaneous state of the network. For an N bus network:

$$V = \overline{V}(k) = \begin{bmatrix} V_1(k) \\ V_2(k) \\ . \\ . \\ V_N(k) \end{bmatrix} \quad (5)$$

For SE, let the N bus voltages, N bus injection currents, and M transmission line currents be respectively measured as Z_i, Z_j, Z_k. Each measurement, except for voltages, is assigned an importance weight and the SE minimizes the weighted least squares performance index:

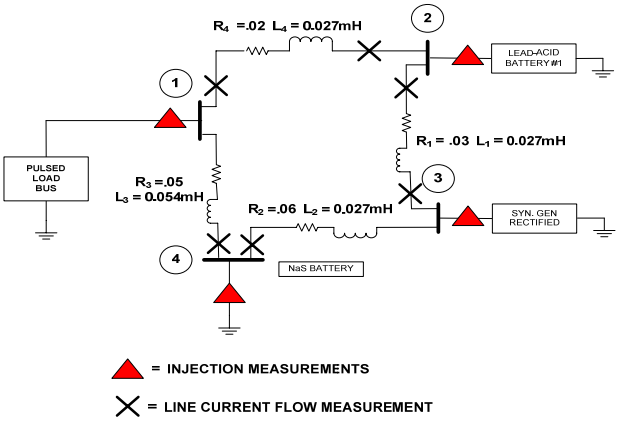

Fig. 2 Pulsed Power 5.7kV dc Loop Network

$$J = \sum_{i=1}^{N}\{V_i - Z_i\}^2 + \sum_{j=1}^{N} U_j\{I_{INJ,j} - Z_j\}^2 + \sum_{k=1}^{2*M} W_k\{I_{LINE,k} - Z_k\}^2 \quad (6)$$

The currents in Eq. (6) are expressed in terms of the voltages and the gradient is set to zero to solve for the state in vector form as a linear equation:

$$\frac{\partial J}{\partial V} = 0 = V - Z_i + \left[\frac{\partial I_{INJ}}{\partial V}\right]^t U\{I_{INJ} - Z_j\} + \left[\frac{\partial I_{LINE}}{\partial V}\right]^t W\{I_{LINE} - Z_k\}$$

$$= V - Z_i + S^t U\{I_{INJ} - Z_j\} + B^t W\{I_{LINE} - Z_k\} \quad (7)$$

In Eq. 7 the matrices S and B are partial derivatives with respect to only the voltage at time step k. Both the injection currents and the line currents depend upon voltages and currents from the previous k-1 sample time as per Eq. 4. The terms on the diagonal of the S matrix are a summation of line current flow terms in the B matrix.

As per Fig.2, the transmission lines are connected 1-2, 2-3, .. where currents are measured into and out of each line. For this example, the 2MxN matrix B has the form:

$$B = \begin{bmatrix} C_1/\Delta t + 1/(R_1 + L_1/\Delta t) & -1/(R_1 + L_1/\Delta t) & 0 & 0 \\ -1/(R_1 + L_1/\Delta t) & C_1/\Delta t + 1/(R_1 + L_1/\Delta t) & 0 & 0 \\ 0 & C_2/\Delta t + 1/(R_2 + L_2/\Delta t) & -1/(R_2 + L_2/\Delta t) & 0 \\ 0 & -1/(R_2 + L_2/\Delta t) & C_2/\Delta t + 1/(R_2 + L_2/\Delta t) & 0 \\ . & . & . & . \\ . & . & . & . \end{bmatrix} \quad (8)$$

The S matrix is NxN with diagonals containing a summation of terms from lines connected to the bus i and $-1/(R_j + L_j/\Delta t)$ on the j^{th} row for a line connected from bus i to bus j.

If all current injection terms are zero, $U_j = 0.0$, there are only line currents measured and voltage vector (where **1** is the identity matrix) is solved for by the equation:

$$\left[1 + S^t U S + B^t W B\right] V = Z_i + B^t W \begin{bmatrix} (C_1 V_1^{k-1} - L_1 I_{1,in}^{k-1})/\Delta t \\ (C_1 V_2^{k-1} - L_1 I_{1,out}^{k-1})/\Delta t \\ (C_2 V_2^{k-1} - L_2 I_{2,in}^{k-1})/\Delta t \\ (C_2 V_3^{k-1} - L_2 I_{2,out}^{k-1})/\Delta t \\ (C_3 V_3^{k-1} - L_3 I_{3,in}^{k-1})/\Delta t \\ (C_3 V_4^{k-1} - L_3 I_{3,out}^{k-1})/\Delta t \\ (C_4 V_4^{k-1} - L_4 I_{4,in}^{k-1})/\Delta t \\ (C_4 V_1^{k-1} - L_4 I_{4,out}^{k-1})/\Delta t \end{bmatrix} + B^t W Z_k \tag{9}$$

When both injection currents and line currents are measured, the optimum voltage vector $\overline{V}$ is obtained from Eq. 7 using the right hand side dependent on prior values and present time samples (*rhs*):

$$\overline{V} = INV * \{rhs\} = \left[1 + S^t U S + B^t W B\right]^{-1} * rhs \tag{10}$$

Accordingly, the best estimate for the measurement vector, $\overline{Z}$, is obtained from the relation [8] derived from SE:

$$\overline{Z} = D\overline{V} = \begin{bmatrix} 1 \\ S \\ B \end{bmatrix} \overline{V} = D \left[D^t \begin{Bmatrix} 1 & 0 & 0 \\ 0 & U & 0 \\ 0 & 0 & W \end{Bmatrix} D \right]^{-1} D^t \begin{bmatrix} Z_i \\ Z_j \\ Z_k \end{bmatrix} \tag{11}$$

Also following the SE derivation, the covariance matrix is:

$$\sum{}^2 = \begin{Bmatrix} 1 & 0 & 0 \\ 0 & U & 0 \\ 0 & 0 & W \end{Bmatrix}^{-1} - \begin{bmatrix} INV & x & x \\ x & S*INV*S^t & x \\ x & x & B*INV*B^t \end{bmatrix} \tag{12}$$

The square root of the nth diagonal of this matrix, Σ_n, is the standard deviation used to normalize the residual of the best estimate and measurement n:

$$\sigma = \left|\overline{z_n} - z_n\right| / \Sigma_n \tag{13}$$

In SE for earth systems operating in steady-state 50 or 60 Hz, the standard deviation is dependent upon the network parameters, topology and independent of weighting factors. Using equations 4 to 12, the definition is modified to be dependent upon instantaneous measurements, the network, and the sampling interval Δt. For non-sampled networks, it has been proven that mixed measurements can be compared, i.e. power and voltages, and the largest among all normalized residuals is the most probable bad data [7]. In subsequent sections it will be demonstrated that the largest normalized residual in Sampled State Estimation (SSE) is also the most probable 'bad data'.

III. A Network Pulse Example

The network of Fig. 2 is to be used as an example of sampled data SE. The lead-acid battery model uses a coefficient $K_c = 1.18$ as a multiplier on the state of charge (SOC), has 2 mOhm resistance, open voltage of 2.135 Volts, for a for a 262 Amp-h battery [9]. The temperature is assumed to be constant 27 degC and there is ~8% voltage drop at full discharge as shown in Fig. 3.

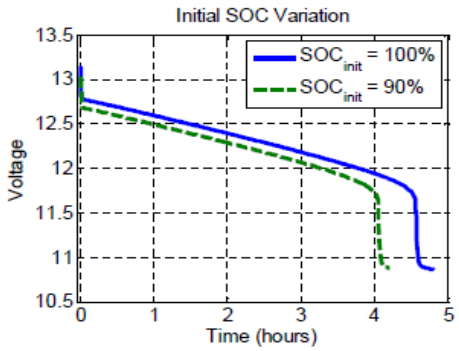

Fig. 3 Lead-acid battery discharge characteristics

The battery is assumed to be fully charged at the start of network transient calculations. The single cell lead-acid characteristics are scaled in parallel and series to obtain a 5500V battery with the same output resistance and 3.1 Amp-h capacity.

To consider another type of energy storage, a Sodium-Sulphur (NaS) battery is shown in Fig. 2. A cell of the NaS battery has the charge/discharge resistance [10] shown in Fig. 4. The characteristics shown in Fig. 4 are scaled to simulate a 5700V, 3.2 Amp-h NaS battery at 300 degC.

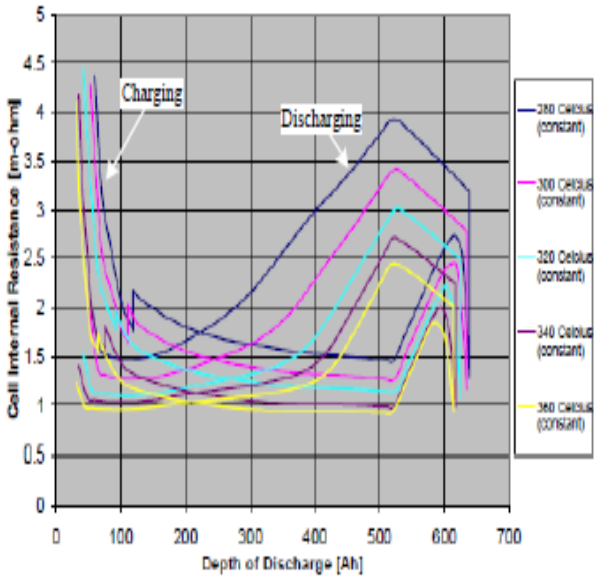

Fig. 4 NaS battery charge and discharge characteristics

At SOC less than 0.65, the NaS terminal voltage decreases 15% as the SOC approaches zero. NaS batteries are already installed on earth power systems for peak shaving, reliability, and to augment capacity of the network [11]. It is questionable whether or not a ship can provide the high temperature environment required to operate NaS batteries.

The 3-phase synchronous generator shown in Fig. 2 is a constant voltage source behind a sub-transient reactance. The output is full wave rectified (6 pulse) to 5500Vdc and has a 1.0mH and 10,000 μF capacitor for an L-C filter on the output.

The R-L transmission lines of the Fig. 2 network have a resistance to inductance ratio:

$$741 \le \frac{R}{L} \le 2222$$

This ratio is representative of insulated conductors in steel conduit as used in ships [12]. Magnitudes of R and L shown in Fig. 2 are selected to demonstrate a large voltage drop from sources to load.

The sources shown in Fig. 2 were triggered to deliver a 3.0 second pulse to the 0.2 Ohm resistive load. The response of the network is shown in Fig.5 where it can be seen that both batteries are depleted after 2.2 seconds. After 2.2 seconds the rectified generator source delivers pulse power. Note that source resistances and transmission line impedances cause considerable voltage drops, such that 5.7 kV sources result in a load voltage less than 4 kV.

The transient at the start of the pulse is shown in Fig. 6. The batteries respond faster than the generator to supply pulse current. Subsequently the sources deliver a maximum ~20,000 Amps to the load at time t = 0.0075 seconds. In general, rotating machines and transformer-coupled converters have slower response than batteries or super capacitors.

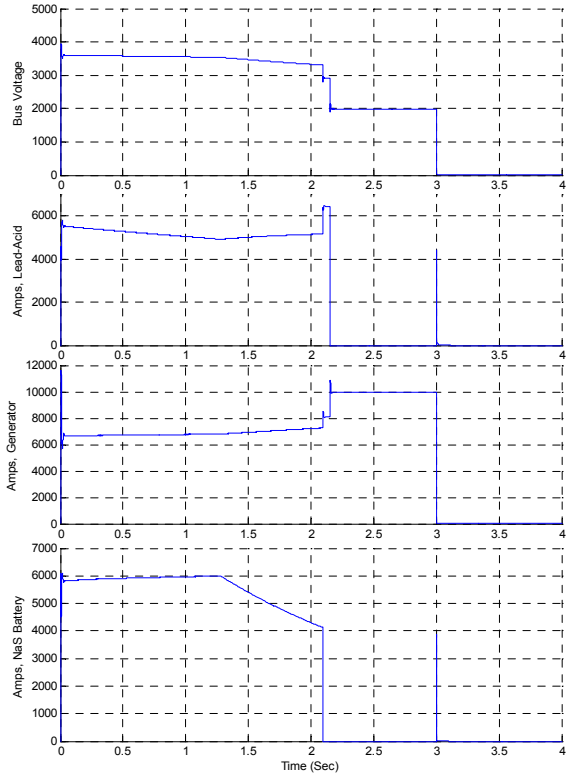

Fig. 5 Pulse response of the Fig. 2 network

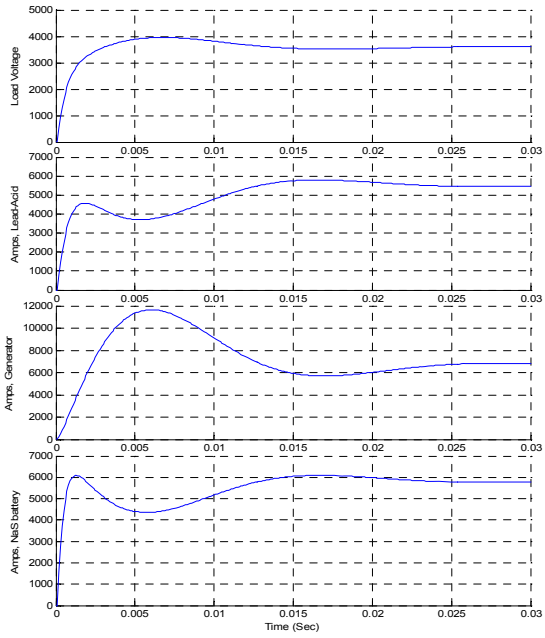

Fig. 6 Initial part of pulse response of the Fig. 2 network

Time	V1	V2	V3	V4	I1	I2	I3	I4	#1in	#2in	#3in	#4in
0.00000	0	0	0	0	-0	0	-0	-0	-0	0	0	-0
0.00050	5496	5005	5700	1614	2499	1139	4430	-8068	-410	730	5159	-2909
0.00100	5493	4626	5696	2551	3992	2797	5966	-12755	-919	1877	7844	-4911
0.00150	5491	4556	5687	3003	4508	4460	6045	-15013	-1561	2899	8945	-6069
0.00200	5491	4586	5685	3264	4562	6005	5752	-16320	-2282	3724	9476	-6844
0.00250	5491	4641	5685	3442	4424	7380	5406	-17210	-3009	4371	9777	-7433
0.00300	5492	4693	5686	3577	4226	8569	5091	-17886	-3697	4873	9963	-7922
0.00350	5492	4729	5687	3685	4031	9566	4829	-18426	-4317	5248	10078	-8348
0.00400	5492	4744	5688	3772	3875	10359	4628	-18861	-4852	5507	10135	-8727
0.00450	5493	4736	5688	3841	3771	10943	4489	-19204	-5291	5652	10141	-9063
0.00500	5493	4713	5689	3892	3721	11334	4405	-19460	-5637	5697	10102	-9358
						During the pulse						
1.50000	5190	3874	5475	3482	4969	6901	5542	-17412	-5855	1045	6588	-10824
1.50050	5190	3875	5474	3482	4968	6902	5541	-17411	-5856	1046	6587	-10824
1.50100	5190	3874	5474	3482	4968	6903	5540	-17411	-5856	1047	6586	-10824
1.50150	5189	3874	5473	3482	4968	6903	5539	-17410	-5856	1047	6586	-10824
1.50200	5189	3874	5473	3482	4968	6905	5537	-17409	-5856	1048	6585	-10824
1.50250	5189	3873	5472	3482	4969	6903	5537	-17409	-5855	1048	6585	-10824
1.50300	5189	3874	5472	3482	4969	6903	5536	-17408	-5855	1048	6584	-10824
1.50350	5189	3874	5471	3481	4968	6904	5534	-17407	-5855	1049	6583	-10824
1.50400	5189	3873	5471	3481	4969	6904	5534	-17407	-5855	1049	6583	-10824
1.50450	5189	3874	5470	3481	4968	6905	5532	-17406	-5855	1050	6582	-10824
1.50500	5189	3873	5470	3481	4969	6905	5532	-17406	-5855	1050	6582	-10824

Table 1 Time snapshots near time t = 0 and time t = 1.5 seconds

IV. Bad Data Detection

If a ship has taken an 'event' that damages part of the power system, or disrupts communications to equipment such as a switchboard, survivability of the ship is at risk. The SE utilizes the redundancy of measurements to calculate the state of the power system to a bus where all measurements are disrupted, in other words, lost. As a general rule, one transmission line flow measurement on each transmission line is sufficient to calculate the state (distant bus voltage) at the far end of a line from the conditions at the local bus, but if the measurement is 'bad', its validity cannot be checked (bad data detected).

Data snapshots are taken on the network and processed by the discrete state estimator algorithm. Samples of the measured voltages and line currents are taken every 0.5 millisecond. Table 1 presents 11 data snapshots at the start of the pulse, Fig. 6, and 11 near the 1.5 second time frame. Each of the snapshots is processed by the algorithm of section III with the weighting factors $U_i = 0.01$, $W_i = 0.1$ However, due to finite difference truncation errors, the minimum standard deviation threshold for bad data detection (residual) of voltages is:

$\sigma_{VThreshold} = 0.6$ Bad data threshold for voltages

Deliberate errors are entered on the data snapshots, and the SSE algorithm is run to find if it can detect the errors. The deliberate errors are created by setting a data point to 0.0 for a voltage or a current reading. The results of the SSE bad data detection are presented in Table 2.

Data point set to zero	Time	Residual
Voltage at bus 3, V3	0.0040	1.21
Voltage at bus 1, V1	0.0020	1.07
Voltage at bus 2, V2	0.0010	1.79
Voltage at bus 2, V2	0.0025	1.65
Voltage at bus 3, V3	0.0025	1.12
Voltage at bus 3, V3	1.5040	1.06
Voltage at bus 1, V1	1.5020	0.95
Voltage at bus 2, V2	1.5010	1.51
Voltage at bus 2, V2	1.5025	1.51
Voltage at bus 3, V3	1.5025	1.06

Table 2. Bad data detection for voltage readings. Single reading set to 0.0 at various times.

In Table 2, every deliberate bad voltage reading is detected and is the largest residual of among all bad data points in its snapshot. When the voltage at bus 3 is set to zero for either the transient time or near t = 1.5 seconds, its normalized residual is 1.21 or 1.26 respectively, which is about twice the bad data threshold, 0.60. Results in Table 2 demonstrate an excellent margin of detection for the point in error. Furthermore, the detected bad data reading is also the largest residual among prior and subsequent snapshots of Table 1.

Because the Euler first order difference scheme truncates the derivative and integral terms, the current weighting factors affect the calculated voltages. To sense bad values in the current snapshot, the weighting factors are adjusted to $U_i = 0.1$ and $W_i = 0.5$ and the minimum standard deviation threshold for bad data detection (residual) for currents is:

$$\sigma_{IThreshold} = 0.7 \text{ Bad Data Threshold for Currents} \quad (20)$$

This bad data threshold for currents is the maximum residual over all data points and all snapshots in Table 1 when there is no fault. A similar test is to be performed on the hardware test bed to determine a threshold.

To test the SSE for detection of bad current data in snapshots, various injection and line currents are arbitrarily set to zero in the snapshot, and the SSE is required to find the bad data point. Results of these tests are presented in Table 3. In Table 3, the snapshot errors are generated by arbitrarily selecting 0.0 as the bad data entry. If the 'real world' data value happens to be near 0.0, then the arbitrary error cannot be detected. An error caused by an algebraic sign change for a sampled data point is a possible alternative test for bad data, but is not used here.

Time	Inj Current set to zero	Residual
0.0025	Im[1], inj. bus 1	0.77
0.0040	Im[2], inj. bus 2	1.16
0.0010	Im[3], inj. bus 3	0.97
0.0010	Im[4], inj. bus 4	2.25
0.0030	Im[3], inj. bus 3	1.00
1.5040	Im[1], inj. bus 1	0.88
1.5025	Im[3], inj. bus 3	1.08
1.5010	Im[4], inj. bus 4	3.17
1.5025	Im[1], inj. bus 2	0.79
1.5040	Im[3], inj. bus 3	1.08

Time	Line Current set to zero	Residual
0.0025	Current into line 3	4.19
0.0040	Current into line 2	1.79
0.0010	Current into line 1	0.74
0.0010	Current into line 3	3.24
0.0030	Current into line 4	2.96
1.5040	Current into line 3	3.02
1.5025	Current into line 2	0.76
1.5010	Current into line 1	1.63
1.5025	Current into line 3	3.02
1.5040	Current into line 4	4.03

Table 3. Bad data detection for current readings. Single reading set to 0.0 at various times.

V. HTSC Line Radial Network

Several energy storage modules and a rectified generator module were simulated in Matlab to create data snapshots for SSE tests on the 7 bus, 6 line dc network of Fig. 6. Two lines are simulated as High Temperature SuperConductor (HTSC) lines with zero resistance, but finite inductance that cannot be eliminated. Each source module is 7.0 kVdc. The HTSC transmission lines comprise a spline network to minimize conduction losses for current delivered to the load.

Because the network is radial, the injection current from each source is also the current into the transmission line from this source. Buses #5 and #6 have zero current injections because they are HTSC connection points. From the first part of the transient, the sampled injection currents at buses 1-4 and bus 7, are presented in Table 4.

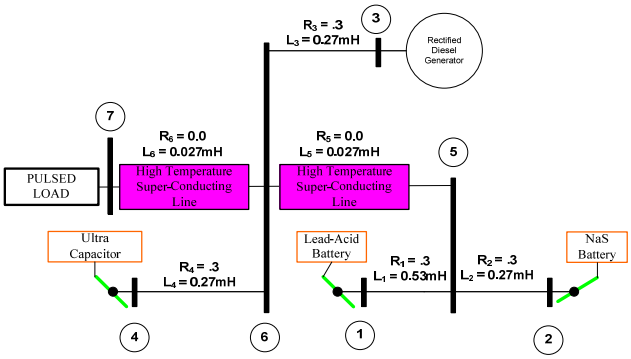

Fig. 6 Line parameters for a HTSC dc radial network

Because the Euler first order difference scheme with a time step 0.0005 seconds truncates the derivative and integral terms, there is a minimum standard deviation threshold for bad data below which errors cannot be detected. For the snapshots of Table 4, in order to detect voltage and line current errors, the weighting factors used are $U_i = 0.0001$ and $W_i = 5.0$. These factors make the detection (residual) of:

$$\sigma_{Threshold} = 0.09 \text{ HTSC bad data threshold} \quad (21)$$

For physical HTSC lines, it is difficult to measure dc currents. The zero resistance of the HTSC lines affects the SSE algorithm because detection of bad data depends on the R and L parameters of a line. Therefore, the line current weighting factors for the HTSC lines are set to a small value $W_i = 0.000001$ to eliminate the HTSC measurements.

Time	V1	V2	V3	V4	V5	V6	V7	Im1	Im2	Im3	Im4	ILOAD
0.00000	0	0	0	0	0	0	0	-0	-0	0	-0	-0
0.00050	6566	7000	6823	6962	4927	4819	4532	1361	2351	2650	2595	-8957
0.00100	6436	6478	7137	6930	5359	5389	5370	1591	2476	4006	2661	-10734
0.00150	6393	5716	7073	6931	5272	5312	5317	1705	1491	4775	2665	-10637
0.00200	6372	5971	6990	6928	5334	5337	5330	1742	1099	5141	2676	-10658
0.00250	6384	6385	6898	6932	5417	5403	5397	1700	1328	5152	2612	-10792
0.00300	6397	6423	6771	6936	5400	5392	5395	1672	1568	4976	2576	-10792
0.00350	6392	6277	6625	6932	5326	5325	5333	1698	1602	4750	2618	-10669
0.00400	6373	6200	6474	6923	5261	5259	5265	1752	1575	4508	2698	-10533
0.00450	6353	6207	6324	6914	5212	5206	5211	1807	1606	4235	2777	-10425
0.00500	6335	6212	6210	6906	5170	5163	5168	1857	1674	3960	2845	-10337
0.00550	6318	6185	6131	6898	5130	5125	5129	1902	1725	3729	2904	-10260
0.00600	6303	6152	6073	6892	5096	5093	5097	1943	1746	3551	2954	-10194
0.00650	6290	6134	6019	6886	5070	5068	5070	1977	1759	3411	2996	-10142
0.00700	6280	6126	5955	6881	5046	5044	5046	2006	1778	3278	3031	-10093
0.00750	6270	6119	5895	6877	5023	5020	5022	2032	1803	3146	3064	-10046
0.00800	6261	6108	5866	6872	5005	5003	5005	2055	1823	3039	3092	-10010
0.00850	6255	6096	5860	6869	4995	4994	4994	2073	1831	2975	3111	-9989
0.00900	6250	6088	5858	6866	4989	4989	4989	2084	1831	2942	3121	-9978
0.00950	6247	6087	5842	6864	4984	4983	4984	2092	1833	2916	3128	-9968

Table 4 Initial data snapshots for HTSC radial network

The SSE algorithm to detect bad data on the network is again tested by means of deliberately setting random data readings to 0.0 at random times. The result of these tests is presented in Table 5. The SSE successfully detects every deliberate bad data point introduced in the snapshots. This summation shows the detected residual is much higher than the minimum threshold. After scanning all data snapshots, a faulty line power to the load. current transducer on line #4, and the SSE presents the summary as:

Done. Worst Resid. = 0.21661 at time .007 Line #4 Flow Cur Meas # 7

Time	Voltage set to zero	Residual
0.0025	Em[1], bus 1	0.81
0.0040	Em[2], bus 2	0.78
0.0010	Em[3], bus 3	0.90
0.0010	Em[4], bus 4	0.84
0.0030	Em[3], bus 3	0.94
0.0070	Em[1], bus 1	0.77

Time	Line Current set to zero	Residual
0.0025	Current into line 3	0.16
0.0040	Current into line 2	0.10
0.0010	Current into line 1	0.10
0.0010	Current into line 3	0.10
0.0030	Current into line 4	0.18
0.0070	Current into line 4	0.22

Table 5 Results of the SSE detecting bad data in the HTSC network

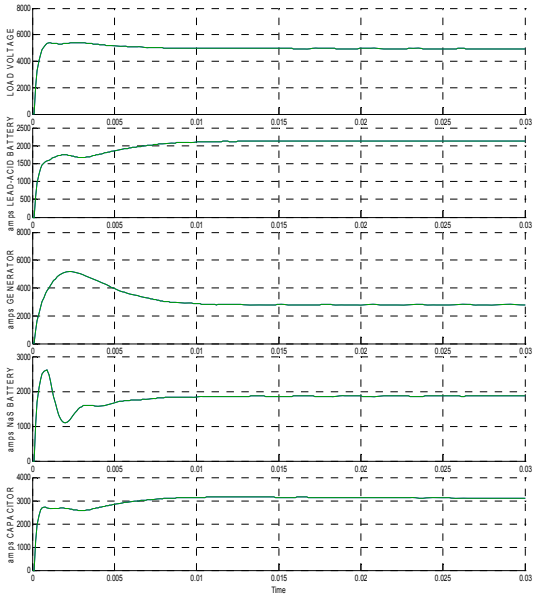

Fig. 7 Initial part of the transient response of the dc HTSC radial network

A design parameter of sampled data systems is frequency of the sampling compared to the time history of the signal. If a signal changes too rapidly compared to the sampling, i.e. the signal has significant frequency components above ½ the sampler frequency, the signal cannot be accurately represented.

VI. CONCLUSIONS

This paper clearly shows the advantages of monitoring a ship's electrical system by Sampled State Estimation (SSE) as driven by a high data rate fiber optic network. The SSE is applicable for any network topology, in both transients and steady state, as demonstrated by the loop and HTSC radial network examples. Data samples from both the initial transient and complete energy pulse have been processed by the SSE to monitor the power system and detect data errors.

Within the proposed sampling time of 0.0005 seconds for the fiber optic network, all SSE functions can be carried out on the central computer, i.e., the Supervisory Control and Data Acquisition (SCADA) computer. Computer timing measurements showed the SSE program code can be executed in <1.0 microsecond, so that larger systems can easily meet the 0.0005 second sampling interval. The 0.0005 sampling time is realizable with existing A/D converters and present-day communications hardware. It is possible to employ a coarser sampling time if anticipated transients are slower than computed for the example networks. Furthermore, the fiber optic network can be used to detect power system network faults within the 0.0005 seconds time frame [13] and implement corrections before the next sample, rather than the of 0.060 seconds, ~ 4 cycles, operation of circuit breakers. Fast fault detection can prevent extensive damage to electronic components and the power network.

Models for four energy storage devices were used in this paper. Further storage development requires actual ship design data such as total energy, discharge voltage, and transmission line parameters from storage to the load. The actual network topology and load cycle of the ship power system are required to locate the distributed energy storage and size the transmission line parameters connecting storage to the load.

With interface modifications, the SSE software can be applied to the actual ship network. It is imperative that physically realizable transmission lines be used in network models. Unrealistic ratios of resistance to inductance, R/L, in other words unrealizable lines, cannot be used in the programs. The HTSC dc radial network required special use of measurement weighting factors for the HTSC lines because they have zero resistance.

VII. REFERENCES

[1] J.F. Dopazo, O.A. Klitin and L.S. Van Slyck, " State Calculations of Power Systems from Line Flow Measurements, Part II", IEE Trans. Power Appar. Syst., Vol. 89, pp 1698-1708, Sept/Nov 1970

[2] G.L. Kusic, "Computer-Aided Power System Analysis", textbook, Prentiss-Hall, 1986

[3] F. Broussolle," State Estimation in Power Systems: Detecting Bad Data Through the Sparse Matrix Inverse Method", IEEE Trans. Power App.. Sys., Vol. PAS-97, pp 678-682, May/June 1978

[4] G.L. Kusic, "Experimental Tests on Power System Monitoring and Fault Detection", report to NASA Glenn Research Center, Task #5 on NAS3-02067, from Power Systems Consultants, Dec 24, 2002

[5] G.L. Kusic, "Power System Fault Detection and Electrical System Monitoring (F-18)", report to Wright-Patterson AFB, Oct 23, 2000

[6] H. Zhao and J. Wu, "Research on a High Energy Utilization Efficiency Electromagnetic Aircraft Launcher with an Ultracapacitor Bank",

[7] M. Ceraolo, "New Dynamical Models of Lead-Acid Batteries", IEEE Trans. Power Sys., Vol.15, No. 4, 2000, pp. 1184-1190

[8] S. Barsali and M. Ceraolo, "Dynamic Models of Lead-Acid Batteries: Implementation Issues", IEEE Trans. Energy Conv., Vol. 17, No. 1, Mar 2002

[9] J.P. Kajs and R.W. Zowarka, "Bus High Current Battery Model", IEEE trans. Magnetics, Vol. 29, No., Jan 1993, pp 1003-1008

[10] A.Attia, G. Halpert, and D. Perrone, "The Development of a Sealed Lead-Acid Battery for Pulse Power Applications", IEEE Proc. 6th Annual battery Conf. on Applic. and Advances, 1991, pp1-19

[11] Z.F. Hussein, et. al.,"Modelling of Sodium Sulphur Battery for Power System Applications", Elektrika, Vol. 9, No. 2, 2007, pp 66-72

[12] LPD17 data from US Naval Surface Warfare Center, Philadelphia, PA 19112

[13] G.L. Kusic, "State Estimation and Fast Fault Detection on Ship Electrical Systems", Electrical Ship Technical Symposium, Arlington, VA May 21-23, 2007, proceedings pages 209-214